SURROGATE MODELLING FOR RISK-TARGETED SEISMIC DESIGN OF ISOLATED STRUCTURES USING FRICTION PENDULUM SYSTEMS

Diego SUAREZ[1], Roberto GENTILE[2] & Carmine GALASSO[3]

Abstract: *Base isolation has been used in the last decades to provide structures with enhanced seismic performance, especially to meet the requirements of risk-critical buildings (e.g., healthcare facilities). This calls for risk-targeted design approaches that consider the explicit computation of various decision variables (e.g., expected annual loss or mean annual frequency of exceeding various damage states). Nonetheless, most of these structures are still designed following implicit risk/reliability considerations derived from building codes. The main hurdle to an explicit risk-based design is the computational effort and time required for seismic performance assessments, given the iterative nature of a typical risk/loss-based design process. This paper proposes using Gaussian-process-regression-based surrogate probabilistic seismic demand models (PSDMs) of equivalent single-degree-of-freedom systems (i.e., the probability distribution of peak horizontal displacements and accelerations on top of the isolation layer conditional on different ground-motion intensity levels) to address these challenges. This enables a risk-targeted methodology for the seismic design of low-rise structures equipped with friction pendulums that virtually requires no design iterations. First, the definition, training, and validation of the surrogate PSDMs are presented. Then, a brief description of a tentative risk-targeted procedure enabled by the proposed surrogate PSDMs is presented. The predictive power of the surrogate PSDMs is verified using a 10-fold cross-validation technique, resulting in normalised root mean square error below 3% for the parameters of the PSDMs and below 7% for their standard deviation.*

Introduction and Motivation

Base isolation is one of the most effective methods for achieving enhanced protection of buildings against the damaging effects of earthquake-induced ground shaking. Base isolation enables superior structural design solutions that meet the needs of risk-aware owners; it is especially adopted for risk-critical facilities such as hospitals, emergency-response buildings, and power-generating stations (e.g., Shao, 2018). Friction Pendulum Systems (FPS) gained much popularity during the last few decades (e.g., Zayas et al. 1990). This technology relies on the friction of a concave surface to achieve seismic isolation and provide restoring forces to the superstructure.

The seismic design of base-isolated structures is commonly carried out by following minimum requirements established in current building codes, such as ASCE 7-10 (ASCE/SEI, 2017) or Eurocode 8 (CEN, 2005). In fact, the intensity-based approach (i.e., a finite number of limit states/performance objectives, each corresponding to a given level of ground-motion intensity) considered in modern seismic codes cannot describe the seismic performance of a building for a full range of ground-shaking intensities and corresponding performance objectives. Probabilistic assessment methods such as the Performance-based Earthquake Engineering (PBEE) approach, as described by the Pacific Earthquake Engineering Research Center (PEER), have been developed to address this. PBEE is the most appropriate approach to calculate decision-variable metrics (i.e., expected annual – monetary – loss) for a given building configuration, including structural and non-structural components (e.g., Moehle and Deierlein, 2004).

Implementing PBEE at the design stage is a challenging task. Indeed, estimating seismic performance involves solving a highly nonlinear problem with various random inputs. This requires the iterative implementation of the PBEE assessment formulation for different structural and non-structural alternatives until a target decision variable value is met. Each iteration of the procedure requires multiple nonlinear time history analyses, thus rendering the design process time- and computational-resource-intensive, arguably incompatible with the preliminary/conceptual design stage. Over recent years, a series of design procedures

[1] Ph.D. student, Scuola Universitaria Superiore IUSS, Pavia, Italy, diego.suarez@iusspavia.it
[2] Assistant Professor, Institute for Risk and Disaster Reduction (IRDR), University College London, UK
[3] Professor, Department of Civil, Environmental and Geomatic Engineering, University College London, UK

incorporating PBEE concepts to obtain risk- or loss-based design have been proposed. Specifically for base-isolated structures, O'Reilly et al. (2022) presented a risk-based method to determine the mean annual probability of exceeding a displacement threshold of the isolation system associated with failure, targeting a maximum displacement reliability value. Other authors (e.g., Hu et al., 2022; Zhang and Huo, 2009) have proposed loss-based design methods relying on advanced optimisation models such as genetic algorithms or multivariate regressions. While the method presented by O'Reilly et al. (2022) provides a closed-form approximation for the risk of failure of FPS, it does not consider seismic losses or other decision variables. Conversely, the second group of approaches require complex computational models and applies to a limited range of structures.

Direct Loss-Based Design (DLBD), first introduced for fixed-based concrete structures (e.g., Gentile and Calvi, 2023; Gentile and Galasso, 2020), represents an appealing risk-targeted design method that does not require design iterations. This approach adopts a flexible and swift mapping between the variables describing inelastic single degree of freedom (SDoF) systems and a selected loss metric. To this aim, a surrogate modelling technique is first used to map different SDoF systems to their probabilistic seismic demand models (PSDMs), describing the probability distribution of various engineering demand parameters (EDPs) conditional to a ground-motion intensity measure (IM). This approach enables computationally-cheap reliability and loss estimates and, consequently, a loss-based design. A designer can, therefore, define a set of seed structural configurations and derive their corresponding loss and structural reliability estimates directly and without iterations. The designer can then select the structure's properties that comply with the required loss target and detail the design accordingly.

This paper presents the development of Gaussian Process (GP) Regression-based surrogate PSDMs towards a DLBD method for base-isolated structures equipped with FPSs. Specifically, two surrogate PSDMs based on GP regressions (e.g., Rasmussen and Williams, 2006), representing the probability distribution of peak horizontal displacements and accelerations on top of the isolation layer conditional on different ground-motion intensity levels, are proposed and validated. Furthermore, a discussion on selecting IMs for which the surrogate PSDMs are conditioned is also included. Finally, a simplified loss/reliability assessment using the surrogate PSDMs is presented and a preliminary DLBD procedure for base-isolated structures is described, highlighting its strengths and limitations.

Surrogated Probabilistic Seismic Demand Models

Two GP regressions (defined below) are used to surrogate the parameters of the PSDMs of SDoF systems representing base-isolated structures (assuming a rigid superstructure). The surrogate models map the SDoF input parameters, $\boldsymbol{X} = \{f_y, t_1, h_{iso}\}$ (i.e., yield strength of the isolation system normalised by the total weight of the structure, f_y; pre-yield period of the SDoF system, t_1; the post-yield to pre-yield stiffness ratio of the isolation system, h_{iso}), to their respective PSDM parameters, $\boldsymbol{Y}_k = \{a_k, b_k, \sigma_k\}$ (i.e., fitting coefficients, a_k, b_k; and lognormal standard deviation, σ_k, of the PSDMs in terms of the specific EDP conditional on the selected IM, where the subscript *k* refers to each of the two PSDMs). The steps for building the surrogate PSDMs are presented below and illustrated in Figure.1.

1. Definition of an SDoF database representing base-isolated structures and described by the parameters in $\boldsymbol{X}$.
2. Selection and scaling of ground motion records and cloud-based nonlinear time history analysis (NLTHA) of each SDoF system from the database.
3. Fitting the PSDMs to the cloud results for each SDoF system, obtaining the PSDMs parameters (defined in the vectors $\boldsymbol{Y}_1$ and $\boldsymbol{Y}_2$).
4. Training the GP-based surrogate PSDMs using the dataset obtained from the cloud-based NLTHAs (Step 3) relating vector $\boldsymbol{X}$ to vectors $\boldsymbol{Y}_1$ and $\boldsymbol{Y}_2$.

Considered PSDMs

The first considered PSDM describes the displacement demand on the isolation system (Δ), and the second represents the peak acceleration demand at the top of the isolation system (A). These models are presented in Eq. 1 and Eq. 2, respectively.

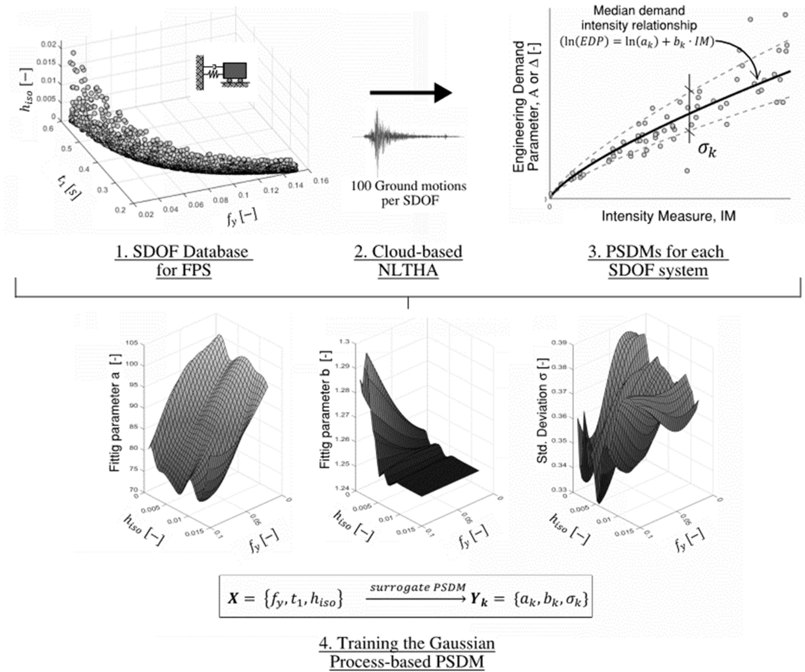

Figure 1. Steps for training the proposed surrogate PSDMs (f_y: yield strength of the isolation system normalised by the total weight of the structure; t_1: pre-yield period of the isolation system; h_{iso}: post-yield to pre-yield stiffness ratio of the isolation system, A: acceleration on top of the isolation system Δ: displacement of the isolation system; a_k, b_k: fitting parameters; σ_k: logarithmic standard deviation of the PSDM).

The PSDMs are obtained by linear regression in the logarithmic space of the IM vs EDP pairs. It is generally suitable for structures with first-mode-dominated responses without strength or stiffness degradation. Each model is characterised by the fitting coefficients, a_k and b_k (describing the mean response), and the dispersion, represented by the logarithmic standard deviation, $\sigma_{\ln(EDP_k)}$ (also referred as σ_k). This model is characterised by homoscedasticity (i.e., constant dispersion over the entire response range) and normally distributed residuals in the logarithmic space (i.e., the residual, ε, is a standard Normal variable).

$$\ln(\Delta) = \ln(a_1) + b_1 \cdot IM + \varepsilon\sigma_{\ln(\Delta)} \quad (1)$$

$$\ln(\mathrm{A}) = \ln(a_2) + b_2 \cdot IM + \varepsilon\sigma_{\ln(\mathrm{A})} \quad (2)$$

SDoF database

A database of 2000 SDoF systems encompasses a wide range of design options representing possible configurations for base-isolated structures using FPSs. To this aim, the SDoF input variables, $\boldsymbol{X} = \{F_y, t_1, h_{iso}\}$, are derived based on the detailing parameters of the isolation system typology (i.e., coefficient of friction and radius of curvature of the sliding surfaces). The modified Bouc-Wen model (Park et al. 1986) describes the hysteresis ($Hyst$) of the FPS, and it is constant for all the SDoFs. A detailed description of the influence of the Bouc-Wen model parameters on the seismic response of base-isolated structures can be found in Ma et al. (2004).

Three parameters define the response of FPS: friction coefficient, μ_{FPS}; the radius of curvature, R_{FPS}; and yield displacement, Δ_y. Those variables are sampled with a plain Monte-Carlo procedure using the ranges of values and distributions shown in Table 1. These values are selected so that there is a comprehensive representation of possible FPS characteristics. The input parameters (f_y , t_1, h_{iso}) are then computed from the sampled values of the random variables by following the general theory of FPSs (e.g., Naeim and Kelly, 1999).

Random Variable	$\boldsymbol{\mu_{FPS}}$ **[%]**	$\boldsymbol{R_{FPS}}$ **[m]**	$\boldsymbol{\Delta_y}$ **[mm]**
Assumed Distribution	$\sim U(1.5,15)$	$\sim U(3,25)$	$\sim U(1.5,2)$

Table 1. SDoF database definition: assumed distributions for the LRB dataset.

Intensity measure selection

The IM used to condition the PSDMs plays a key role in the accuracy of the loss/reliability calculations. The selected IM should lead to small record-to-record variability (efficiency) and should lead to structural response estimates that are independent of other ground-motion parameters, such as magnitude and source-to-site distance (sufficiency), as has been noted in previous works (e.g., Ebrahimian and Jalayer, 2021). Any IM can be selected for the analysis, assuming that site-specific hazard curves can be computed in terms of the selected IM. This work uses peak ground velocity (or PGV); this selection is based on the computability of this IM and on an efficiency analysis (e.g., Luco and Cornell, 2007) on SDoF systems, although not shown here for brevity. A more extensive discussion on IM selection for base isolated structures using FPSs can be found, for example, in Cardone et al. (2017).

Seismic response analysis

For each SDoF system in the database, 100 ground motion records are used to perform cloud-based NLTHA. The ground motions are selected from the SIMBAD database (Selected Input Motions for displacement-Based Assessment and Design) developed by Smerzini et al. (2014). These recorded ground motions are characterised by moment magnitudes in the range of 5-7.3, source-to-station distances smaller than 35km and peak ground acceleration values in the range of 0.29g -1.77g. However, users can re-fit the surrogate model by considering any set of ground motions (by filtering the existing results or by running NLTHA for different sets of records).

The ground motion records are linearly scaled so that there is adequate sampling of displacement demand values while using reasonable scaling factors, i.e., as close to the unity as possible, to avoid biases in the seismic demand estimation (e.g., Dávalos and Miranda, 2019). To do so, 100 equally-spaced (tentative) displacement targets are sampled between 0 and 0.6m. Then, for each tentative displacement target, a response reduction factor is computed according to Eq. 3 derived by Zhou F and L. (2003), where ξ is the equivalent viscous damping at the displacement target. The required elastic spectral displacement at the isolated period of the SDoF system, $SD(t_{iso})_{req}$, is calculated as $SD(t_{iso})_{req} = \Delta_{target}/\eta$. Finally, a required scaling factor is computed for each ground motion in the database as $SF = SD(t_{iso})_{req}/SD(t_{iso})$. Consequently, the ground motion with the smallest required scaling factor is selected and used for each NLTHA. It is assumed that each selected ground motion can be used a maximum of two times within the cloud analysis. Note that the NLTHA will not result exactly in the assumed displacement value since the response reduction factors are based on empirical approximations for highly damped systems. The resulting scaling factors range from 0.4 to 2.5.

$$\eta = 1 + \frac{0.05 - \xi}{0.06 + 1.4 \cdot \xi} \quad (3)$$

Training of the surrogate models

GPs are statistical distributions over functions, entirely defined by their mean and covariance functions (e.g., Rasmussen and Williams, 2006). A GP regression involves conditioning a prior GP (in a Bayesian framework) to an input-output training dataset (in this case, ***X*** and ***Y*** previously defined). GP regressions are non-parametric statistical models and, therefore, not constrained to any specific functional form. The user only needs to define the typology of the covariance function (e.g., Rasmussen and Williams, 2006). For this work, a squared exponential covariance function is used since it can model the expected smoothness of the input-output map (i.e., a small perturbation of the input SDoF parameters causes a small variation of the PSDM parameters). The parameters of the covariance function are called hyperparameters, and they are calibrated using a maximum likelihood approach and a quasi-Newton optimisation method. The assumptions adopted for the training process are consistent with those implemented by Gentile and Galasso (2022), where they are more extensively explained.

Validation of the Gaussian Process Regression

Once the proposed surrogate models have been trained, the normalised root mean squared error (NRMSE) is calculated according to Eq. 4 to assess the predictions within the dataset. In Eq. 4, s_h represents the predicted outputs (e.g., the PSDM parameters) and m_h are the modelled outputs for the *h*-th input vector. The NRMSE values for the displacement surrogate PSDMs of parameters a_1, b_1, and σ_1 are 1.3%, 2.4% and 6.8%, respectively. For the acceleration surrogate PSDMs, the NRMSE values of parameters a_2, b_2, and σ_2 are 0.6%, 3.3% and 8.8%, respectively.

$$NRMSE = \frac{mean(\sqrt{(s_h - m_h)^2})}{mean(m_h)} \quad (4)$$

To assess the predictive power of the surrogate models for unseen data (i.e., generalisation outside of the training dataset), a 10-fold cross-validation is performed. To this aim, the dataset is first randomly divided into ten equally-sized subsets. Then, ten more GP regressions are fitted for each surrogate model by leaving out one subset at a time and using the remaining nine subsets for the training. The excluded subset is used as a testing benchmark for each GP regression to compute the in-fold predicted-vs-modelled errors. Finally, the in-fold NRMSE is calculated by aggregating the predicted-vs-modelled errors of the 10 GP regressions.

The in-fold NRMSE values for the parameters *a, b,* and *σ* of the displacement PSDMs are equal to 1.6%, 2.6% and 7.2%, respectively. For the acceleration PSDMs, the analogous NRMSEs are equal to 0.6%, 3.5% and 9.2% (see Figure 2). Therefore, given the uncertainties commonly involved in the seismic performance assessment and risk models, the error introduced by using the provided GP regressions is deemed acceptable.

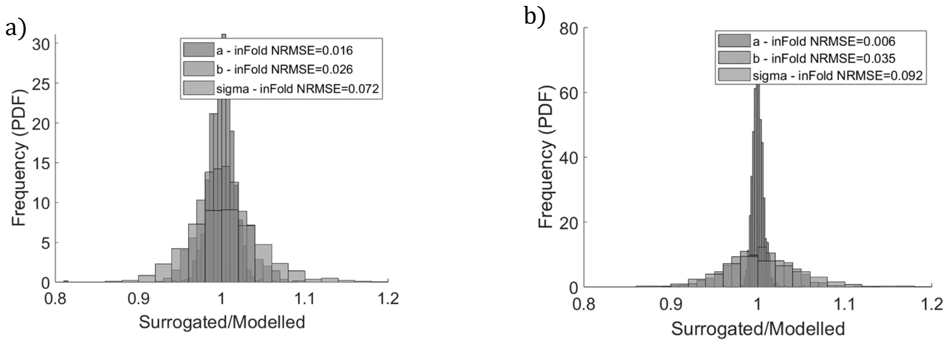

Figure 2. Surrogated (GP regression) versus modelled (SDoF cloud analysis) points; a) displacement PSDM and b) acceleration PSDM.

Simplified reliability and loss assessment

This section illustrates the use of the proposed GP regressions to compute reliability and loss metrics for a base-isolated structure by separately analysing four subsystems (Figure 4): isolation system, superstructure, drift-sensitive (NSCD) and acceleration-sensitive non-structural components (NSCA). This section adopts direct economic losses for the description, although other loss metrics may be adopted (e.g., downtime). The reliability metrics are computed by deriving fragility curves (representing the probability of being in or exceeding a certain damage state given the IM level) for various damage states (DSs) of interest. For this description, the selected reliability metrics are the mean annual frequency of exceedance (MAFE) of the near-collapse DS of the isolation system (defined as the exceedance of a displacement threshold corresponding to the FPS displacement capacity) and the MAFE of the yielding DS for the superstructure. A vulnerability model for each subsystem (representing the mean repair cost normalised by the total reconstruction cost, or loss ratio, for a given IM level) is computed separately and aggregated to obtain the selected building-level loss metric. The selected loss metric for this section is the Expected Annual Loss (EAL).

A site-specific hazard model, described by hazard curves (expressing the MAFE of the IM, λ_{IM}), in terms of the selected IM required by the surrogate PSDMs, is adopted. The hazard curves can be obtained from ready-available models (e.g., Meletti et al. 2006) or computed by performing probabilistic seismic hazard analysis (e.g., Cornell 1968).

Vulnerability model of the isolation system

The displacement surrogate PSDM (Eq. 1) is used to derive lognormal fragility curves, F_{DS_i}, for the isolation system, which are computed for predefined DSs. Although other definitions are possible, the recommended DSs are inspection and near collapse (Suarez et al., 2023). Their respective damage state thresholds Δ_{DS_i} can be set according to the client´s inspection requirements and aided by the experience and judgment of the designer. The fragility curves are fully characterised by their median, η_{DS}, and logarithmic standard deviation, β, which are calculated as shown in Eq. 5.

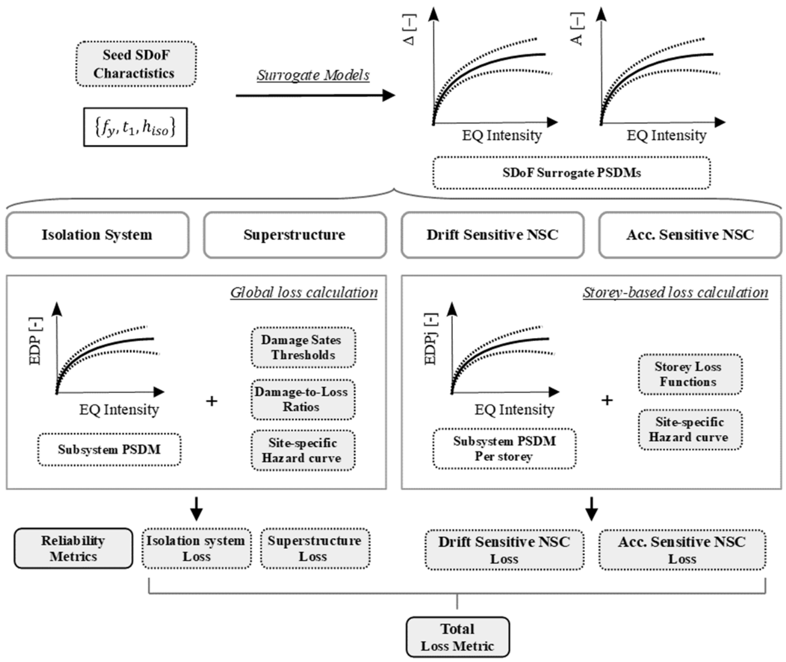

Figure 3. Simplified loss and reliability assessment module.

$$\eta_{DS_i} = \sqrt[b_1]{\frac{\Delta_{DS_i}}{a_1}}\ ;\ \beta = \sigma_1 \tag{5}$$

The vulnerability model for the isolation system, $LR_{iso}(IM)$, is computed through Eq. 6. This requires using damage-to-loss ratios for each DS, DLR_{DSi}, which represent the mean loss ratio constrained on the realisation of the *i-th* DS. Those can be obtained based on expert/engineering judgement and/or catalogues of FPS.

$$LR_{iso}(IM) = \sum_{i=1}^{\#DS+1} \left(F_{DS_{i-1}}(IM) - F_{DS_i}(IM)\right) DLR_{DSi} \tag{6}$$

Vulnerability model of the superstructure

The superstructure response (i.e., maximum storey drifts and peak floor accelerations) conditioned on the IM is estimated based on the surrogate PSDMs (Eq. 1 and Eq. 2) and relying on an elastic modal response analysis of a two-degree-of-freedom (2DoF) model (Naeim and Kelly, 1999). The approximation assumes that the response of the base-isolated structure is completely described by its fundamental mode of vibration. The 2DoF model is composed of two equivalent SDoF systems in series, the isolation system and the (elastic) superstructure (Figure 4). The properties of the 2DoF model are derived based on the effective (i.e., consistent with the maximum response) properties of the structure.

A yield displacement profile for the superstructure is selected according to displacement-based design principles (Priestley et al., 2007), and then the properties of a substitute SDoF system are computed. Specifically, the effective yield displacement, $\Delta_{y,e}$; effective mass, m_e; and effective height, h_e of the substitute structure are calculated according to Eq. 7. $\Delta_{y,j}$ is the assumed displacement at the *j-th* storey in yielding conditions, h_j is the height of the *j-th* storey and m_j is the mass at the *j-th* storey.

$$\Delta_{y,e} = \frac{\sum_{j=1}^{N}(m_j \cdot {\Delta_{y,j}}^2)}{\sum_{j=1}^{N}(m_j \cdot \Delta_{y,j})}\ ;\ m_e = \frac{\sum_{j=1}^{N}(m_j \cdot \Delta_{y,j})}{\Delta_{y,e}}\ ;\ h_e = \frac{\sum_{j=1}^{N}(m_j \cdot \Delta_{y,j} \cdot h_j)}{\sum_{j=1}^{N}(m_j \cdot \Delta_{y,j})} \tag{7}$$

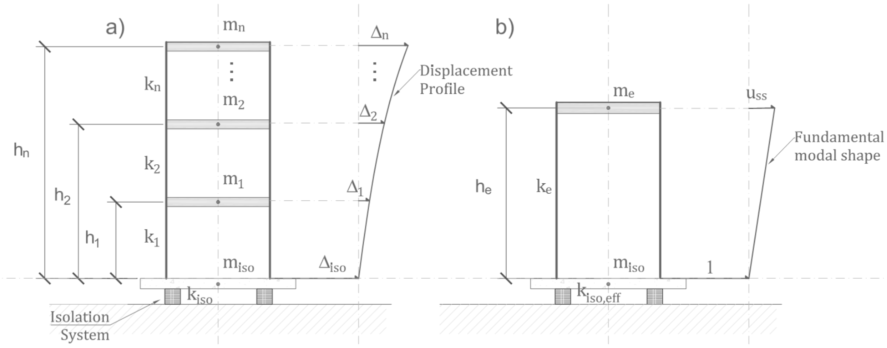

Figure 4. a) Multi-degree-of-freedom model for a base-isolated structure. B) 2DoF model representation and its fundamental modal shape neglecting higher order mode effects.

The relative displacement of the superstructure with respect to the isolation system, Δ_{SS}, is computed according to Eq. 8. $\mathrm{U}_{SS}(\mathrm{IM})$ defines the mode shape of the 2DoF as per Figure 4 and it is computed with Eq. 9. (Ye et al. 2019). T_{eff} is the fundamental period of the isolation system (assuming a rigid superstructure) and computed using its effective stiffness corresponding to a maximum displacement conditioned on IM and described by the surrogate PSDM (Eq. 1); T_{SS} is the fundamental period of the fix-based configuration of the superstructure; m_T is the total mass of the isolated structure and m_{iso} is the mass of the isolation layer. The ductility demand on the superstructure conditioned on the IM is finally calculated as $\mu_{SS}(IM) = \Delta_{\mathrm{SS,e}}(\mathrm{IM})/\Delta_{y,e}$.

$$\Delta_{\mathrm{SS}}(\mathrm{IM}) = \Delta(\mathrm{IM})\mathrm{U}_{SS}(\mathrm{IM}) \tag{8}$$

$$U_{SS}(\mathrm{IM}) = \left(\frac{T_{SS}}{T_{eff}(IM)}\right)^2 \cdot \frac{m_T}{m_{iso} + m_e} \tag{9}$$

The parameters for the lognormal fragility curves of the superstructure are computed according to Eq. 10, which is derived by combining Eq. 1 and Eq. 8. The vulnerability model for the superstructure is computed analogously to Eq. 6 for the isolation system and adopting appropriate DSs and DLRs defined in terms of the ductility demand of the superstructure. The suggested DSs -and related DLRs- are, for example, slight and moderate damage (defined as in Gentile and Calvi, 2023).

$$\eta_{DS_i} = \sqrt[b_1]{\frac{\Delta_{DS_i} \cdot \varepsilon_{eq}}{a_1 \cdot \Delta_{y,e}}}\ ;\ \beta = \sigma_1 \tag{10}$$

Vulnerability model of non-structural component groups

The acceleration at the isolation base is directly derived using the acceleration surrogate PSDM (Eq. 2). The acceleration at the effective height of the superstructure, A_{SS}, is estimated with Eq. 11.

$$\mathrm{A}_{SS}(IM) = \mathrm{A}(\mathrm{IM}) \cdot (1 + \mathrm{u}_{SS}(\mathrm{IM})) \tag{11}$$

The PSDMs for the non-structural components (NSCs), describing the maximum inter-storey drift $\theta_i(IM)$ and peak floor acceleration $PFA_i(IM)$ values conditioned on IM at each storey, are calculated according to appropriate acceleration and displacement profiles for the superstructure and the expressions derived by Eq. 8 and Eq. 11.

The loss calculation for NSCs is based on the abovementioned PSDMs and storey loss functions, SLFs (Ramirez and Miranda, 2009). SLFs relate the EDP experienced at a specific storey to a loss metric. SLFs must be previously defined for each storey of the structure, separately for acceleration- and drift-sensitive NSCs. One option to obtain SLFs involves a simulation-based approach in which, for a given potential inventory of non-structural components and their respective fragilities models, several loss simulations are performed for different levels of EDPs demands, and an SLF is then fitted to this data by assuming a probability distribution, i.e., Papadopoulos et al. (2019).

Once the SLFs are defined, they are combined with the inter-storey drift and the peak floor acceleration PSDMs to obtain storey-based vulnerability models for NSCs. The total vulnerability models for NSCD and NSCA are computed by aggregating the vulnerability models of each storey,j, as shown in Eq. 12 and Eq. 13, respectively.

$$LR_{NSCD}(IM) = \sum_{i=1}^{n} SLF_j(\theta_j(IM)) \tag{12}$$

$$LR_{NSCA}(IM) = \sum_{i=0}^{n} SLF_j(PFA_j(IM)) \tag{13}$$

Building-level loss and reliability metrics

The loss metric for each subsystem *n* is computed as the convolution of the vulnerability model for the subsystem, $LR_n(IM)$, with the site-specific hazard curve, as per Eq. 14. Finally, the losses for the four subsystems are aggregated to obtain the total EAL (Eq. 15).

$$\mathrm{EAL_n} = \int_0^{\infty} LR_n(IM) \left|\frac{d\lambda_{IM}}{dIM}\right| dIM \tag{14}$$

$$EAL = \sum_{n=1}^{4} EAL_n \tag{15}$$

The selected reliability metric corresponding to the MAFE of the near-collapse DS of the isolation system, $\lambda_{iso_{NC}}$ is computed according to Eq. 16, where $F_{NC}(IM)$ is the fragility curve for the near collapse DS. The MAFE of the yielding DS of the superstructure, $\lambda_{ss_{yield}}$ is computed analogously.

$$\lambda_{iso_{NC}} = \int_0^{\infty} F_{NC}(IM) \left|\frac{d\lambda_{IM}}{dIM}\right| dIM \tag{16}$$

Tentative Direct Loss-based design procedure

This section provides a tentative DLBD procedure for low-rise buildings equipped with FPSs (Figure 4). DLBD allows the designing of a building (isolation system and superstructure) that achieves a selected *loss target* for a site-specific seismic hazard profile. The loss target, L_{target}, (e.g., 0.02% EAL) is defined (by the client and/or designer) consistently with the loss metric computed with the simplified loss and reliability assessment module described above. An additional design criterion involves imposing a selected minimum level of reliability. For example, this may be achieved by imposing an upper bound for the MAFE of the near-collapse DS of the isolation system, $\lambda_{iso_{NC}}$ and an upper bound limit for the MAFE of the DS related to the yielding of the superstructure, $\lambda_{yield_{SS}}$. DLBD virtually does not require design iterations due to the simplified nature of the loss and reliability calculations.

From a high-level point of view, DLBD starts by identifying a set of seed structures using different combinations of *design parameters* of the isolation system (weight normalised yield strength, f_y; fundamental period, t_1; and hardening ratio, h_{iso}) and the superstructure (weight normalised superstructure yield strength, $f_{y_{SS}}$). The simplified loss and reliability assessment module (fully automated) is run for all the seed structures at a remarkably low computational cost. The seed structures that comply with the design requirements (Eq. 17) are equally valid design candidates. Finally, a design solution is arbitrarily chosen among the candidates based on user/client preferences, as well as gravity-load design requirements. Structural detailing, strictly not part of DLBD, allows the detailing of the final structure in compliance with the parameters of the design solution (including isolation parameters and force-displacement curve of the superstructure).

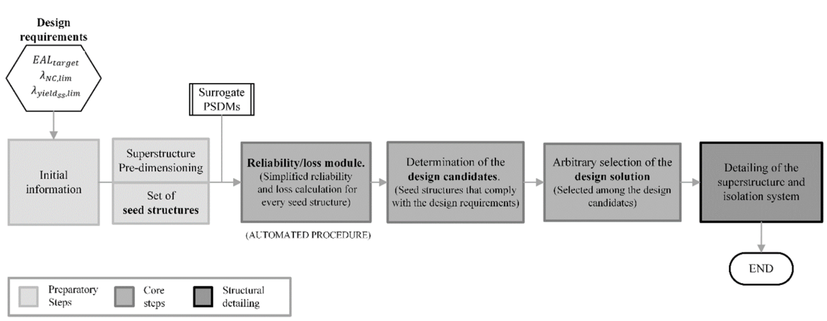

Figure 5. Workflow for the DLBD procedure. Taken from Suarez et al., 2023.

A preliminary validation study (Suarez et al., 2023) involves a three-storey medical clinic with an RC wall lateral resisting system for the superstructure and lead rubber-bearing base isolation. The structure is in a high-seismicity region and is designed to achieve a target EAL equal to 0.017% of the total reconstruction cost, considering direct losses only. Although the validation study is being refined and enlarged, the preliminary results show a 9.6% relative error of the target EAL with respect to refined NLTHA-based results. Even though direct-only economic loss may not be the most appropriate loss type to consider for isolated structures, the preliminary results show that the procedure is dependable, and it is worth extending it to include more-relevant loss metrics such as downtime.

Conclusions

This paper presented the formulation, calibration, and verification of two surrogate probabilistic seismic demand models (PSDMs) based on Gaussian Process (GP) regressions. Those allow estimating the probability distribution of the displacement demand and the peak acceleration demand of single-degree of freedom (SDoF) systems representing structures equipped with friction pendulum base isolation systems. A database of cloud-based nonlinear time-time history analyses for 2000 SDoF systems was used to calibrate the GP regressions. A 10-fold cross-validation showed adequate prediction capacity of the adopted GP regressions: normalised mean squared errors below 3% for the parameters of the PSDMs and below 7% for their standard deviation.

The proposed surrogate PSDMs enabled the tentative proposal of a Direct Loss-based Design (DLBD) of base-isolated structures. This procedure allows designing structures that would achieve, virtually without design iterations, a given economic loss target for a given site-specific hazard profile while complying with a predefined minimum level of structural reliability. A general overview of the tentative DLBD procedure for base-isolated structures was presented. Some remarks about this work are summarised in the following:

- Surrogate models based on GP regressions represent an appealing tool to generate predictions of PSDMs.
- The proposed surrogate PSDMs effectively and efficiently overcome the high computational cost required to derive numerical fragility models for several seed design configurations (otherwise incompatible with the preliminary design phase).
- The estimation errors of the proposed surrogate PSDMs lie within acceptable ranges, especially considering the uncertainties and approximations generally affecting seismic risk analyses.
- The proposed tentative DLBD procedure is currently under more detailed scrutiny and validation to overcome some identified limitations. For example, the adopted SDoF assumption only allows capturing the first mode response of the combined isolation and superstructure system. This implies that the superstructure's maximum acceleration and displacement response are assumed in phase with the isolation layer. As a result, DLBD loses its effectiveness for less-desirable configurations where higher modes are important. This may be overcome by imposing a high relative stiffness of the superstructure with respect to the effective stiffness of the isolation system. Moreover, in highly damped isolated systems, the coupling of modal shapes can generate high floor accelerations response (Skinner et al., 1993) that are currently not captured in the proposed procedure.

References

ASCE/SEI, 2017. Minimum design loads for buildings and other structures. ASCE/SEI 7-16. VA, USA.

Cardone, D., Lucchini, A., Mastrangelo, E., Mollaioli, F., 2017. Seismic Response Prediction of Spatial Base-Isolated Structures, IJREAT International Journal of Research in Engineering & Advanced Technology.

CEN, 2005. Eurocode 8: Design of structures for earthquake resistance, EN 1998. Brussels.

Cornell, C.A., 1968. Engineering seismic risk analysis. Bulletin of the Seismological Society of America 58, 1583–1606. https://doi.org/10.1785/BSSA0580051583

Dávalos, H., Miranda, E., 2019. Evaluation of bias on the probability of collapse from amplitude scaling using spectral-shape-matched records. Earthq Eng Struct Dyn 48, 970–986. https://doi.org/10.1002/eqe.3172

Ebrahimian, H., Jalayer, F., 2021. Selection of seismic intensity measures for prescribed limit states using alternative nonlinear dynamic analysis methods. Earthq Eng Struct Dyn 50, 1235–1250. https://doi.org/10.1002/eqe.3393

Gentile, R., Calvi, G.M., 2023. Direct loss-based seismic design of concrete structures. Earthquake Engineering & Structural Dynamics, under rev.

Gentile, R., Galasso, C., 2020. Gaussian process regression for seismic fragility assessment of building portfolios. Structural Safety 87, 101980. https://doi.org/10.1016/j.strusafe.2020.101980

Luco, N., Cornell, C.A., 2007. Structure-specific scalar intensity measures for near-source and ordinary earthquake ground motions. Earthquake Spectra 23, 357–392. https://doi.org/10.1193/1.2723158

Meletti, C., Meletti, C., Stucchi, M., Stucchi, M., 2006. Database della pericolosità sismica MPS04.

Moehle, J., Deierlein, G.G., 2004. A framework methodology for performance-based earthquake engineering.

Naeim, F., Kelly, J., 1999. Design of seismic isolated structures: from theory to practice. John Wiley & Sons, New York.

O'Reilly, G.J., Yasumoto, H., Suzuki, Y., Calvi, G.M., Nakashima, M., 2022. Risk-based seismic design of base-isolated structures with single surface friction sliders. Earthq Eng Struct Dyn. https://doi.org/10.1002/eqe.3668

Papadopoulos, A.N., Vamvatsikos, D., Kazantzi, A.K., 2019. Development and application of FEMA P-58 compatible story loss functions. Earthquake Spectra 55, 95–112. https://doi.org/10.1193/102417EQS222M

Park, Y.J., Wen, Y.K., Ang, A.H.-S., 1986. Random vibration of hysteretic systems under bi-directional ground motions. Earthq Eng Struct Dyn 14, 543–557. https://doi.org/10.1002/eqe.4290140405

Priestley, M., Calvi, G., Kowalsky, M., 2007. Displacement-Based Seismic Design of Structures.

Ramirez, C.M., Miranda, E., 2009. Building-specific loss estimation methods & tools for simplified performance-based earthquake Engineering.

Rasmussen, C.Edward., Williams, C.K.I., 2006. Gaussian processes for machine learning. MIT Press.

Shao, B., 2018. Toward Performance-based Design of Seismically Isolated Structures.

Skinner, R.I., Robinsson, W.H., McVerry, G.H., 1993. An Introduction to Seismic Isolation. John Wiley & Sons Ltd, West Sussex .

Smerzini, C., Galasso, C., Iervolino, I., Paolucci, R., 2014. Ground motion record selection based on broadband spectral compatibility. Earthquake Spectra 30, 1427–1448. https://doi.org/10.1193/052312EQS197M

Suarez, D., Rubini, G., Gentile, R., Galasso, C., 2023a. Gaussian process regression-based surrogate modelling for direct loss-based seismic design of low-rise base-isolated structures. Procedia Structural Integrity 44, 1728–1735. https://doi.org/10.1016/j.prostr.2023.01.221

Ye, K., Xiao, Y., Hu, L., 2019. A direct displacement-based design procedure for base-isolated building structures with lead rubber bearings (LRBs). Eng Struct 197. https://doi.org/10.1016/j.engstruct.2019.109402

Zayas, V.A., Low, S.S., Mahin, S.A., 1990. A Simple Pendulum Technique for Achieving Seismic Isolation. Earthquake Spectra 6, 317–333. https://doi.org/10.1193/1.1585573

Zhou F, W., L, X.Z., 2003. State of the art on applications, R&D and design rules for seismic isolation in China., in: Proc. 8th World Seminar on Seismic Isolation, Energy Dissipation and Active Vibration Control of Structures. Yerevan, Armenia.